

DETECTION OF PULSED X-RAY EMISSION FROM PSR B1706–44

E. V. GOTTHELF,¹ J. P. HALPERN,¹ R. DODSON²

Submitted to The Astrophysical Journal Letters

ABSTRACT

We report the first detection of pulsed X-ray emission from the young, energetic radio and γ -ray pulsar PSR B1706–44. We find a periodic signal at a frequency of $f = 9.7588088 \pm 0.0000026$ Hz (at epoch 51585.34104 MJD), consistent with the radio ephemeris, using data obtained with the High Resolution Camera on-board the *Chandra X-ray Observatory*. The probability that this detection is a chance occurrence is 3.5×10^{-5} as judged by the Rayleigh test. The folded light curve has a broad, single-peaked profile with a pulsed fraction of $23\% \pm 6\%$. This result is consistent with the *ROSAT* PSPC upper limit of $< 18\%$ after allowing for the ability of *Chandra* to resolve the pulsar from a surrounding synchrotron nebula. We also fitted *Chandra* spectroscopic data on PSR B1706–44, which require at least two components, e.g., a blackbody of $T_\infty = (1.66_{-0.15}^{+0.17}) \times 10^6$ K and a power-law of $\Gamma = 2.0 \pm 0.5$. The blackbody radius at the nominal 2.5 kpc distance is only $R_\infty = 3.6 \pm 0.9$ km, indicating either a hot region on a cooler surface, or the need for a realistic atmosphere model that would allow a lower temperature and larger area. Because the power-law and blackbody spectra each contribute more than 23% of the observed flux, it is not possible to decide which component is responsible for the modulation in the spectrally unresolved light curve.

Subject headings: pulsars: individual (PSR B1706–44) — stars: neutron — X-rays: stars

1. INTRODUCTION

PSR B1706–44 is a 102 ms radio pulsar discovered by Johnston et al. (1992) and possibly associated with the supernova remnant G343.1–2.3 (McAdam, Osborne, & Parkinson 1993). With characteristic age $P/2\dot{P} = 17,500$ yr and spin-down luminosity $\dot{E} = 3.4 \times 10^{36}$ ergs s^{–1} PSR B1706–44 is considered a young, energetic neutron star. The distance to the pulsar is somewhat uncertain. According to the Taylor & Cordes (1993) free electron model of the Galaxy the pulsar lies 1.8 kpc away, however Koribalski et al. (1995) find a kinematic distance in the range 2.4 – 3.2 kpc from H I absorption. Originally detected as the high-energy γ -ray source 2CG342–02 by the *COS B* satellite (Swanenburg et al. 1981), PSR B1706–44 is one of approximately eight rotation-powered pulsars that are responsible for some of the brightest γ -ray sources in the sky. Thompson et al. (1992; 1996) showed that photons detected from the direction of PSR B1706–44 by the EGRET instrument on board the *Compton Gamma-Ray Observatory* are pulsed at the radio period. All of the known γ -ray pulsars are well observed at X-ray energies between 0.1 and 10 keV, where both surface thermal emission and magnetospheric synchrotron emission can be studied. However, *pulsed* X-ray emission has not been detected from PSR B1706–44 despite several searches. This failure has hindered attempts to understand its X-ray emission mechanism(s).

Using an observation of PSR B1706–44 by the *ROSAT* PSPC, Becker, Brazier, Trumper (1995) placed an upper limit of 18% on the pulsed fraction. They attributed this negative result to the diluting effect of an as-yet unresolved synchrotron nebula, recalling the history of Vela (Ögelman, Finley, & Zimmerman 1993), a pulsar of similar

age and spin-down luminosity. Finley et al. (1998), using data from the *ASCA* GIS, placed an upper limit of 22% on the pulsed fraction in the 2–10 keV band, although their image was severely contaminated by stray light from the bright low-mass X-ray binary 4U1705–44 just outside the field of view. Finley et al. also analyzed a *ROSAT* HRI observation, from which they concluded that $57 \pm 12\%$ of the photons associated with PSR B1706–44 actually come from a compact nebula with an exponential scale length of $\approx 27''$. When folding only the photons from the HRI point source at the radio period, they derived an upper limit of 29% on its pulsed fraction. An observation by the non-imaging *Rossi X-ray Timing Explorer* performed during a low state of 4U1705–44 also failed to detect pulsations in the 9–18.5 keV band. (Ray, Harding, & Strickman 1999). Here we report on *Chandra* observations of PSR B1706–44 in which we detect its pulsed emission in X-rays.

2. OBSERVATIONS

The field of PSR B1706–44/G343.1–2.3 was observed by *Chandra* twice, once with each of the two types of cameras at the focal plane of the telescope. Herein we analyze data from these observations, made available through the *Chandra* public archive.

Timing data on PSR B1706–44 were acquired on 2000 Feb 11 with the imaging High Resolution Camera (HRC-I; Murray et al. 1997), a multichannel plate detector with an effective time resolution degraded to ~ 4 ms due to a known timing error. The HRC is sensitive to X-rays in the energy range 0.1 – 10 keV; no useful spectral information is available. The target was placed near ($\approx 28''$) the optical axis where the telescope mirror point-spread function (PSF) has half power radius (the radius enclosing 50% of the total source counts) of $\sim 0.5''$ for energies

¹Columbia Astrophysics Laboratory, Columbia University, 550 West 120th Street, New York, NY 10027

²School of Mathematics and Physics, University of Tasmania, GPO Box 252–21, Hobart, Tasmania 7001, Australia

$E < 6$ keV. The HRC-I oversamples the PSF with pixels $0.''1318$ on a side, which allows the pulsar to be isolated from any surrounding emission such as the pulsar wind nebulae (PWNe) typically found associated with young pulsars observed by *Chandra* (e.g., see Gotthelf 2001).

Data were also obtained with the Advanced CCD Imaging Spectrometer (ACIS; Burke et al. 1997), which has resolution $\Delta E/E \sim 0.1$ at 1 keV scaling as $1/\sqrt{E}$ over its 0.2–10 keV active band-pass. The pulsar was observed on 2000 Aug 14 and positioned on the back-illuminated S3 chip of the ACIS-S array, offset by $0.''5$ from the aim-point, where the PSF is undersampled by the $0.''4920 \times 0.''4920$ CCD pixels. Data were collected in the nominal timing mode, with 3.241 s exposures between CCD readouts, and in “FAINT” spectral mode.

The standard *Chandra* screening criteria produced a total usable exposure time of 46.8 ks and 14.3 ks for the HRC and ACIS data sets, respectively. These resulted in a similar number of detected photons from the source, and the images made from the two instruments are found to be consistent. The ACIS image, restricted to the 0.3 – 8 keV energy band to reduce instrumental background, reveals a point-like X-ray source at the radio pulsar position and four nearby faint X-ray sources that are coincident with USNO stars to sub-arcsecond accuracy. The *Chandra* position of PSR B1706–44 is $\alpha = 17^{\text{h}}09^{\text{m}}42^{\text{s}}.73$, $\delta = -44^{\circ}29'08''.4$ (J2000.0) with RMS error $0.''5$. This is in agreement with the precise radio timing position of Wang et al. (2000, see Table 1).

To look for evidence of extended emission around PSR B1706–44 we constructed a radial profile, the distribution of counts per unit area in the HRC as a function of distance from the pulsar. For comparison, we analyzed a 23 ks *Chandra* observation of the millisecond pulsar PSR J0437–4715 observed at the aim-point of the HRC just two days later (Zavlin et al. 2002). PSR J0437–4715 is an isolated point source with a spectrum similar to that of PSR B1706–44 (as shown in §4), thus providing a realistic example of the in-orbit point-spread function. Figure 1 displays the two radial profiles after adjusting for different background intensities, sampled in an annulus of $30'' < r < 60''$ where the background is flat. We then normalized the two profiles to the peak intensity within $r < 1.''0$. While the majority of the emission is point-like, there is clearly diffuse emission out to a radius of $\approx 20''$. There is also a bump of enhanced emission between $11'' < r < 23''$. This result is consistent with the analysis of these data by Dodson & Golap (2002), who displayed extended emission out to $\approx 5''$, and is marginally consistent with the decomposition of the *ROSAT* HRI image deduced by Finley et al. (1998). In order to make a direct comparison with the *ROSAT* energy band, we also extracted photons from the ACIS image in the range 0.2 – 2.0 keV. After background subtraction, we find 513 photons in the ACIS from the point source (radius $1.''5$), and 383 nebular photons in the annulus $1.''5 < r < 20''$.

3. TIMING ANALYSIS

We searched for a pulsed signal from PSR B1706–44 in the HRC data using time-tagged photon events extracted from an $3.''0$ radius aperture centered on the X-ray pulsar position. This aperture effectively excludes most of the dif-

fuse emission from the putative surrounding synchrotron nebula; furthermore, less than 3% of the photons in this aperture are background events. The arrival times of the 824 selected photons were corrected to the solar system barycenter using the JPL-DE200 ephemeris and the radio timing position. We then generated a periodogram using the Z_1^2 statistic (Rayleigh test) on a range of test frequencies centered on the predicted pulsar frequency derived from a fit to radio observations from the Parkes Observatory archives (Wang et al. 2000) that span the X-ray observation. The residual deviations of the radio pulse arrival times from the fitted quadratic ephemeris in Table 1 are less than 1 ms, including one observation that occurred 24 days before the X-ray observation. The known dispersion measure was used to correct the radio pulse arrival times to infinite frequency for absolute phase comparison with the X-ray pulse.

The X-ray periodogram is shown in Figure 2. We find a peak at $f = 9.7588088 \pm 0.0000026$ Hz (epoch 51585.34104 MJD) which, within the quoted 68% uncertainty range, is identical to the contemporaneous radio frequency, $f = 9.7588097$ Hz. The Z_1^2 statistic for this peak is 20.54, which has a probability of chance occurrence of 3.5×10^{-5} . The light curve, shown in Figure 3, is broad and single peaked with a pulsed fraction of $23\% \pm 6\%$. According to convention, the pulsed fraction is defined as the ratio of counts above the minimum in the light curve to the total counts. This detection is consistent with the previous upper limits of $< 29\%$ from the *ROSAT* HRI (Finley et al. 1998) and $< 18\%$ from the *ROSAT* PSPC (Becker et al. 1995). The latter did not resolve the pulsar from the nebula, therefore, it represents a true upper limit of $< 31\%$ given the contribution of diffuse photons measured in the *Chandra* ACIS image as described in §2. The arrival time of the radio pulse is consistent with occurring at the center of the broad X-ray peak. This is not the case for the EGRET γ -ray pulse, which is centered ≈ 0.37 cycles after the radio pulse (Thompson et al. 1996).

4. SPECTROSCOPY

To characterize the energy dependence of the emission from the pulsar and its putative wind nebula, we analyzed spectral data obtained with the ACIS detector. Pulsar and PWN source counts spectra were extracted from two concentric regions, a circle of radius $1''$ and an annulus of radii $2'' < r < 10''$, respectively. An annular background region centered on the pulsar was extracted from radii $30'' < r < 60''$, which appears to be pure background (see Fig. 1). We verified that background is a negligible contribution to the pulsar spectrum and a 10% contribution to the PWN spectrum over their respective extraction regions. To be specific, there are 561(486) source counts and an estimated 1(54) background count(s) for the pulsar(PWN) regions in the 0.5 – 8.0 keV spectral fitting range. From the radial profile (Fig. 1) it is clear that there is negligible cross-contamination between the pulsar and PWN extraction regions.

The ACIS pulse-height data were corrected for gain and resolution degradation due to CCD charge transfer inefficiencies (CTI) using the *correctit* software (Townesley et al. 2001). We used the supplied instrument response matrices appropriate for the CTI corrected data. Since the location of the target on the CCD straddled regions covered

by two response files, we generated a count-weighted mean response to match the data. The CIAO tool `mkarf` were used to generate a point-source mirror response matrix for the pulsar and PWN source regions. The extracted photons were binned in pulse-height channel space to match the response matrices and regrouped such that each fitted spectral bin contained a minimum of 20 counts. The resulting spectra were then fitted with the X-ray spectral analysis package `XSPEC` (version 11.1) using three different models, a power law, a simple blackbody, and a sum of both, each with interstellar absorption.

Initial fits to the pulsar spectrum using blackbody or power-law models were unacceptable, with $\chi^2 = 115$ and $\chi^2 = 60$ for 23 degrees-of-freedom (DoF), respectively. We next determined, as is often the case for young pulsars, that a blackbody plus power-law fit provides an adequate description of the spectrum. The intrinsic parameters of this multicomponent model are rather unconstrained and strongly correlated with the fitted value of the interstellar absorption column density, N_{H} . To remove an unnecessary degree of freedom, we fixed N_{H} at the value obtained from a simple fit to the PWN, $5.5 \times 10^{21} \text{ cm}^{-2}$, since we expect the intervening column density to be the same. The PWN is well characterized by a single absorbed power-law with $\chi^2 = 13$ for 20 DoF. The results of these fits are given in Table 2, and the counts spectrum of the pulsar, with the model components superposed, are shown in Figure 4.

The fitted blackbody component yields effective temperature $T_{\infty} = (1.66^{+0.17}_{-0.15}) \times 10^6 \text{ K}$, bolometric luminosity $L_{\infty} = 6.8^{+0.8}_{-1.1} \times 10^{32}$, and effective radius $R_{\infty} = 3.6 \pm 0.9 \text{ km}$ in the observed frame. Here we adopt a distance of 2500 pc as a compromise between the smaller DM distance of 1.8 kpc, and the H I kinematic distance of 2.4 – 3.2 kpc. While T_{∞} is consistent with some standard neutron star cooling curves (Umeda, Tsuruta, & Nomoto 1994), the associated R_{∞} is significantly smaller than theoretical neutron star radii. As has been found frequently for other pulsars, e.g., Vela (Pavlov et al. 2001), such an outcome could have either of two implications. First, the thermal X-rays could be coming from a smaller hot region on the surface of a cooler neutron star, the substantial interstellar N_{H} making it difficult to measure softer X-rays coming from the full surface. Second, a more realistic atmosphere model, especially if dominated by hydrogen or helium, would require a lower effective temperature and larger effective radius, perhaps becoming consistent with emission from the full neutron star surface.

5. DISCUSSION AND CONCLUSIONS

There are at least two mechanisms for the emission of broad-band pulsed X-rays from young rotation-powered pulsars like PSR B1706–44. One is non-thermal magnetospheric synchrotron from relativistic electrons and positrons created either in regions above the neutron star polar caps or in outer gaps. The second is thermal emission from the hot surface, a result of initial cooling of the hot neutron star or reheating of the polar caps by back-flowing accelerated particles. Sometimes the shape of the

pulse sheds additional light on the X-ray emission mechanism. Sharp, narrow pulses of high amplitude can only be produced by a highly beamed, thus relativistic population of electrons, while quasi-sinusoidal pulses of low amplitude such as describe PSR B1706–44 can be produced by either mechanism. For those intermediate-age pulsars ($10^4 - 10^6 \text{ yr}$) that are also EGRET sources, the presence of both types of X-ray source is usually discovered when spectrally resolved timing data are available (e.g., Wang et al. 1998; Pavlov et al. 2001). Unfortunately, in this case, the *Chandra* HRC has little or no energy resolution. Since each spectral component fitted to the ACIS spectrum contributes more than 23% of the flux in the total energy band to which the HRC is sensitive (60% from blackbody, 40% from power law), the pulsed fraction alone does not reveal the source of the pulsed X-rays. Either or both components may contribute to the modulation. Future spectrally resolved X-ray observations with high throughput and moderate time resolution, such as with *XMM-Newton*, could resolving this ambiguity.

The $> 100 \text{ MeV}$ luminosity of most γ -ray pulsars is a significant fraction of their spin-down power. In the case of PSR B1706–44 this fraction is ≈ 0.20 if isotropic, while its $0.5 - 8 \text{ keV}$ non-thermal X-ray luminosity is only $1.3 \times 10^{-4} \dot{E}$ including both pulsar and nebula, similar to that of other pulsars. Thompson et al. (1996) parameterized the EGRET spectrum of PSR B1706–44 as a broken power law, with photon index $\Gamma = 1.27 \pm 0.09$ from 50 MeV to 1 GeV, steepening to $\Gamma = 2.25 \pm 0.13$ above 1 GeV. Since there is no evidence for any *unpulsed* γ -ray emission, the EGRET spectrum can be compared directly with the power-law component of the pulsar point source in the *Chandra* ACIS spectrum. When extrapolated back to 10 keV, the EGRET spectrum nearly matches the X-ray flux, although the power-law X-ray slope itself, with $\Gamma = 2.0 \pm 0.5$, is somewhat steeper than the EGRET value. The non-thermal X-rays are not likely to be emitted by the same population of electrons/positrons as produce the γ -rays, but may instead originate from a much less energetic population, such as secondary pairs from the inward emitted γ -rays converting on the strong B -field near the neutron star surface. This distinction is also supported by the observed phase offset between the X-ray and γ -ray pulses (§3). The Wang et al. (1998) model predicts L_x (2–10 keV) $\approx 2 \times 10^{31} \text{ ergs s}^{-1}$ and $\Gamma = 1.5$ from this process for PSR B1706–44, which is similar to its observed non-thermal X-ray component. If its *thermal* luminosity comes partly from a small surface area, then inward flowing primary electrons impacting the polar caps may be responsible. Wang et al. predicted $L_x \approx 1 \times 10^{33} \text{ ergs s}^{-1}$ of thermal emission from this process, not far from the observed thermal luminosity of PSR B1706–44.

This work made use of data obtained from the *Chandra* Data Archive, and is supported by NASA LTSA grant NAG 5-7935 to EVG. We thank D. Lewis and R. N. Manchester for their assistance with the radio ephemeris.

REFERENCES

- Becker, W., Brazier, K. T. S., & Trümper, J. 1997, *A&A*, 298, 528
- Burke, B. E., Gregory, J., Bautz, M. W., Prigozhin, G. Y., Kissel, S. E., Kosicki, B. N., Loomis, A. H., & Young, D. J. 1997, *IEEE Transac. Elec. Devices*, 44, 1633
- Dodson, R., & Golap, K. 2002, *MNRAS*, submitted
- Finley, J. P., Srinivasan, R., Saito, Y., Hirayama, M., Kamae, T., & Yoshida, K. 1998, *Ap. J.*, 493, 884
- Gotthelf, E. V. 2001, in “Proceedings of the Texas Relativistic Astrophysics Meeting,” Austin, Texas (astro-ph/0105128)
- Johnston, S., Lyne, A. G., Manchester, R. N., Kniffen, D. A., D’Amico, N., Lim, J., & Ashworth, M. 1992, *MNRAS*, 255, 401
- Kaspi, V. M., Bailes, M., Manchester, R. N., Stappers, B. W., Sandhu, J. S., Navarro, J., & D’Amico, N. 1997, *ApJ*, 485, 820
- Koribalski, B., Johnston, S., Weisberg, J. H., & Wilson, W. 1995, *ApJ*, 441, 756
- McAdam, W. B., Osborne, J. L., & Parkinson, M. L. 1993, *Nature*, 361, 516
- Murray, S. S., et al., 1997, *SPIE*, 3114, 11
- Ögelman, H., Finley, J. P., & Zimmerman, H. U. 1993, *Nature*, 361, 136
- Pavlov, G. P., Zavlin, V. E., Sanwal, D., Burwitz, V., & Garmire, G. P. 2001, *ApJ*, 552, L129
- Ray, A., Harding, A. K., & Strikman, M. 1999, *ApJ*, 513, 919
- Swanenburg, B. N., et al. 1981, *ApJ*, 243, L69
- Taylor, J. H., & Cordes, J. M. 1993, *ApJ*, 411, 674
- Thompson, D. J., et al. 1992, *Nature*, 359, 615
- Thompson, D. J., et al. 1996, *ApJ*, 465, 385
- Townsley, L. K., Broos, P. S., Garmire, G. P. & Nousek, J. A. 2000, *ApJ*, 534, L139
- Umeda, H., Tsuruta, S., & Nomoto, K. 1994, *ApJ*, 433, 256
- Wang, F. Y.-H., Ruderman, M., Halpern, J. P., & Zhu, T. 1998, *ApJ*, 498, 373
- Wang, N., Manchester, R. N., Pace, R. T., Bailes, M., Kaspi, V. M., Stappers, B. W., & Lyne, A. G. 2000, *MNRAS*, 317, 843
- Zavlin, V. E., Pavlov, G. G., Sanwal, D., Manchester, R. N., Trümper, J., Halpern, J. P., & Becker, W. 2002, *ApJ*, 000, L000 (astro-ph/0112544)

TABLE 1
RADIO EPHEMERIS OF PSR B1706–44

Parameter	Value
R.A. (J2000)	17 ^h 09 ^m 42. ^s 728
Decl. (J2000)	–44°29′08.″24
Valid Range (MJD)	51520 – 51956
Epoch (MJD) ^a	51585.3410392671
Frequency (Hz)	9.7588096779
Frequency Derivative (Hz s ^{–1})	–8.880796 × 10 ^{–12}
Dispersion Measure (cm ^{–3} pc)	75.69

^aTDB epoch of radio peak at infinite frequency.

TABLE 2
SPECTRAL FITS TO PSR B1706–44 AND ITS PWN^a

	Pulsar	Nebula
N_{H} (10 ²¹ cm ^{–2})	5.5 (fixed)	5.5 ^{+2.5} _{–2.1}
Γ	2.0 ^{+0.5} _{–0.5}	1.34 ^{+0.24} _{–0.30}
C_{pl}^{b}	4.3 ^{+3.1} _{–1.6} × 10 ^{–5}	5.5 ^{+2.6} _{–1.8} × 10 ^{–5}
$F_{\text{pl}}(\text{absorbed})^{\text{c}}$	1.2 × 10 ^{–13}	3.4 × 10 ^{–13}
$L_{\text{pl}}(\text{unabsorbed})^{\text{d}}$	1.45 ^{+0.46} _{–0.08} × 10 ³²	3.1 ^{+1.5} _{–1.0} × 10 ³²
T_{∞} (K) ^e	1.66 ^{+0.17} _{–0.15} × 10 ⁶	...
R_{∞} (km) ^e	3.6 ± 0.9	...
L_{∞} (ergs s ^{–1}) ^e	6.8 ^{+0.8} _{–1.1} × 10 ³²	...
χ^2_{ν} [DoF]	1.4 [21]	0.61 [21]

^aUncertainties are 68% confidence for two interesting parameters.

^bPower-law normalization in units of photons cm^{–2} s^{–1} keV^{–1} at 1 keV.

^cPower-law flux (ergs cm^{–2} s^{–1}) in the 0.5–8 keV band.

^dPower-law luminosity (ergs s^{–1}) in the 0.5–8 keV band for $d = 2500$ pc.

^eSpherical blackbody parameters for $d = 2500$ pc.

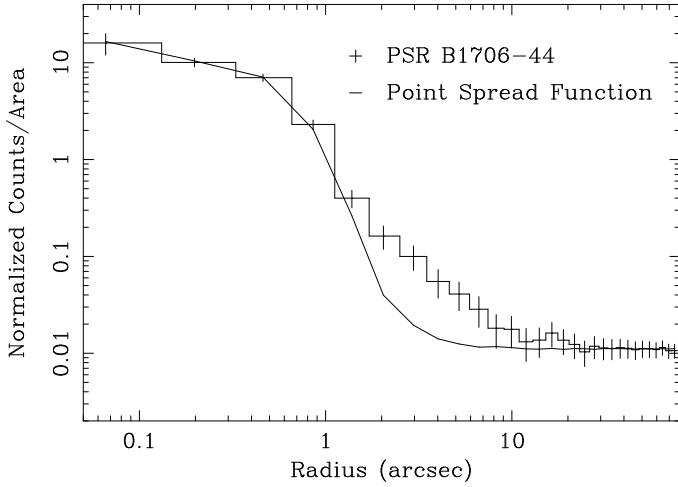


FIG. 1.— X-ray intensity of PSR B1706–44 as a function of radius measured with the *Chandra* HRC (histogram), compared with the HRC response to a point source (solid line; see text). The radial profile shows clear evidence for extended emission between $1''.5$ and $20''$. The error bars are 1σ .

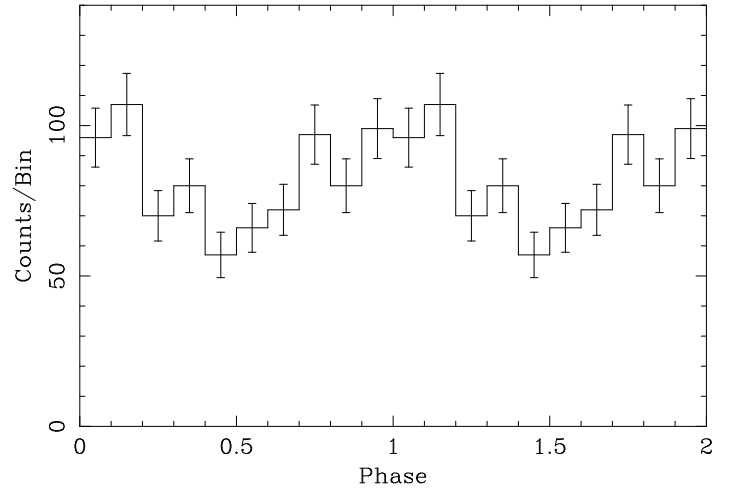


FIG. 3.— The light curve of PSR B1706–44 from the *Chandra* HRC folded according to the radio ephemeris of Table 1. The quasi-sinusoidal modulation has pulsed fraction of $23\% \pm 6\%$. Phase zero corresponds to the epoch of the radio peak. The error bars are 1σ .

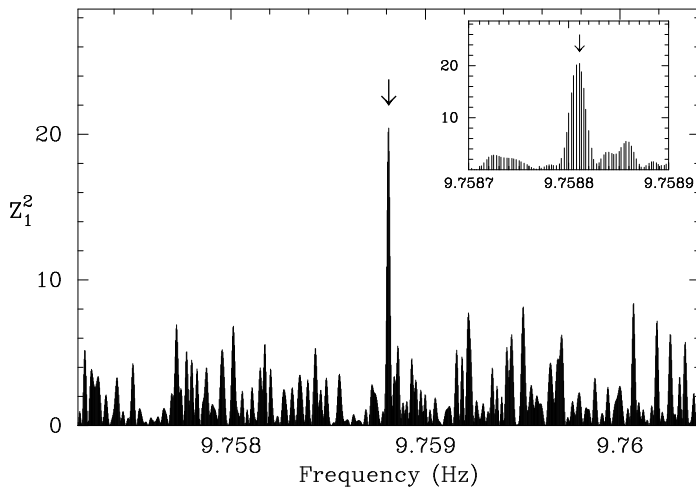


FIG. 2.— Evidence for pulsed X-ray emission from PSR B1706–44 using a Z_1^2 periodogram. The arrow indicates the frequency expected according to the extrapolated radio ephemeris (see text). The inset is an expanded view around the peak. The peak value $Z_1^2 = 20.54$ at $f = 9.7588088$ Hz has a 3.5×10^{-5} probability of occurring by chance.

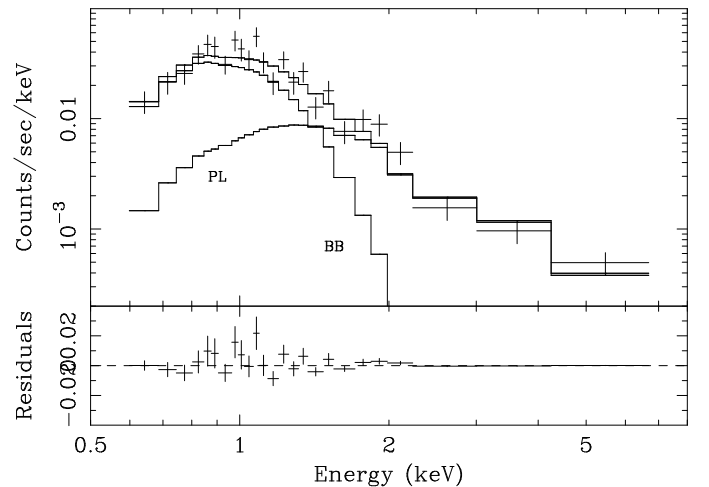


FIG. 4.— *Chandra* ACIS-S3 spectrum of the point source coincident with PSR B1706–44. *Top panel*: Data (crosses) and best-fit model (dark line) for the parameters given in Table 2; thin lines show the contribution of the power-law (PL) and blackbody (BB) components of the fit. *Bottom panel*: Difference between the data and model, in the same units as the top panel.